

Supplement of Atmos. Chem. Phys., 15, 8401–8421, 2015
<http://www.atmos-chem-phys.net/15/8401/2015/>
doi:10.5194/acp-15-8401-2015-supplement
© Author(s) 2015. CC Attribution 3.0 License.



Supplement of

Aerosol chemistry above an extended archipelago of the eastern Mediterranean basin during strong northern winds

E. Athanasopoulou et al.

Correspondence to: E. Athanasopoulou (eathana@phys.uoa.gr)

The copyright of individual parts of the supplement might differ from the CC-BY 3.0 licence.

1 **S1 Supplementary model details**

2 The meteorological inputs for the PMCAMx applications are provided by the WRF/ARW model
3 (Skamarock et al. 2008) (<http://www.wrf-model.org/index.php>). The model is driven by the National
4 Centers for Environmental Prediction (NCEP) operational Global Final (FNL) Analyses (1.0°×1.0°
5 spatial resolution), in combination with Sea Surface Temperature (SST), from the Real-Time Global
6 SST (0.5°×0.5° spatial resolution). The 25-category USGS land-use classification scheme was adopted
7 in order to provide land-cover data. The planetary boundary layer (PBL) parameterization used is the
8 ‘first-order’ closure scheme developed by the Yonsei University (YSU) (Hong et al., 2006). This
9 scheme was selected as it is non-local and has a better performance than other schemes as far as water
10 vapor mixing ratio predictions are concerned (Dandou et al. 2014), which is an important input
11 parameter for air quality studies (Tombrou et al. 2015).

12 The WRF numerical simulations were performed using triple two-way nesting, with the first domain
13 covering the extended area of Europe (23.0 to 77.0°N, 14.5 to 44.5°E) with 0.5° horizontal resolution,
14 the second covering the extended area of Greece and Italy (29.3 to 50.2°N, 4.8 to 32.2°E) with 0.167°
15 horizontal resolution and the third following the horizontal grid system as PMCAMx. In the vertical
16 axis, 35 full sigma levels resolve the atmosphere (model top at 50hPa or 20 km), with a finer
17 resolution near the surface.

18 The global model GEOS-CHEM (Bey et al., 2001; <http://acmg.seas.harvard.edu/>) is applied in order to
19 cope with the transported air masses from outside the PMCAMx simulation domain. The model is
20 driven by assimilated meteorological data from the Goddard Earth Observing System, Version 5
21 (GEOS-5) of the NASA Global Modeling and Assimilation Office (<http://gmao.gsfc.nasa.gov>). The
22 version applied for the current study (v8-03-01) uses the SOA chemical mechanism, which includes
23 the NO_x-O_x-hydrocarbon-aerosol species module and a SOA module based on the framework
24 proposed by Chung and Seinfeld (2002) and Henze et al. (2008). Moreover, the ISORROPIA II
25 package for aerosol thermodynamical equilibrium is used (Fountoukis and Nenes, 2007).

26 A 9-month (January to September 2011) simulation of the global model is initially performed (4°
27 latitude × 5° longitude). Three-hour boundary conditions (BCs) are calculated for May-September
28 2011 (allowing 5-month model spin up) around a domain centered in Europe (22 to 74° N and -20 to
29 45° E). A previous study over the same area of interest (Tombrou et al., 2009) has shown the
30 importance of a nested GEOS-CHEM application in order to provide initial and boundary gaseous
31 concentrations to a regional air quality model during summertime. Thus, a nested run over this
32 window is applied, with 0.5° (latitude) × 0.67° (longitude) horizontal resolution (Protonotariou et al.,
33 2013). The vertical grid is composed by 47 levels up to 0.01 hPa.

34

35 **S2 Emission model inputs**

1 The PMCAMx applications are provided with hourly emissions for a series of pollutants from different
2 source categories. Data for the area of Greece include NO_x, SO₂, NMVOC, CO, NH₃ and bulk PM₁₀
3 emissions from several types of industries, road transport, central heating, maritime activities,
4 railways, air traffic, agricultural activities and isoprene, terpenes, NO from forests (provided by the
5 Ministry of Environment for the year 2002). This emission database has been refined to account for
6 the changes related to the newer motor highway inside the Athens basin. These emissions vary against
7 season and weekday/weekend of the week.

8 In the frame of this study, emission rates for the area of Turkey are retrieved from the EMEP emission
9 dataset (<http://www.ceip.at/webdab-emission-database/officially-reported-emission-data/>). NO_x, SO_x,
10 NMVOC, CO, NH₃ PM_{2.5} and PM_{coarse} emissions from the 10 recommended SNAP sectors at 0.5° x
11 0.5° are horizontally downscaled to the model grid following the land use (eg. coarse ship emissions
12 are equally split only to the fine cells covered by the sea). The vertical downscaling of the EMEP
13 emissions for PMCAMx is done using the disaggregation factors proposed by Bieser et al. (2011), as
14 described in Mailler et al. (2013). The temporal disaggregation of the EMEP emissions from the yearly
15 totals to hourly values for a winter and a summer weekday and weekend is performed using the
16 temporal factors extracted from Greek National emissions.

17 The daily emission rates from anthropogenic and natural sources of gaseous and particulate
18 atmospheric constituents used in the PMCAMx model are given in Table S1. The emissions of most
19 species in the two countries are in similar levels (e.g., nitrogen species are ca. 50 megaton/day).
20 Differences (e.g. in particulate sulfate) are attributed to difference in the surface coverage between the
21 two countries, and the fact that a significant part of Istanbul (and emission sources therein) is outside
22 the PMCAMx simulation domain (treated as BCs by GEOS-CHEM). At this point, it should be noted
23 that particulate sulfate is the most abundant anthropogenic emitted specie. This is in line with the
24 significance (above 60%) of the industrial contribution in PM₁₀ emissions in Athens and Istanbul
25 reported in Kanakidou et al. (2011) and explains the predominance of sulfate in the total aerosol
26 content in the EM (Kopanakis et al., 2012; Im et al., 2012; Tagaris et al., 2013).

27 Sea-salt particles, road (tire, brake, road wear and re-suspension) and soil dust emission fluxes are
28 calculated online with meteorology, following the methodology developed and applied by
29 Athanasopoulou et al. (2008, 2010). The size and chemical distribution of total aerosol emissions to
30 the species and size bins used by the current PMCAMx model applications are also described therein.
31 An update is related with the conversion of organic carbon (OC) to total organic aerosol (OA). In
32 particular, industrial and motorway OC emissions are multiplied by a factor of 1.25 and by 1.54,
33 respectively (Bergstrom et al., 2012; Brown et al., 2013), so that the modeled organic concentrations
34 are directly comparable to the measured organic mass. The chemical speciation of the non-methane
35 hydrocarbons from transportation and industry for SAPRC99 is described in Bossioli et al. (2002).

1 The emission databases used for the GEOS-CHEM applications are from fossil fuel burning (including
2 ships) from the EMEP inventory for the European domain (Vestreng and Klein, 2002), biofuel
3 emissions (Yevich and Logan, 2003), biogenic VOC emissions from vegetation based on the MEGAN
4 model (Guenther et al., 2006) and natural sources from the oceans (Spracklen et al., 2008), volcanic
5 activity (Chin et al., 2000) and lightning (Price and Rind, 1992). Global biomass burning emissions are
6 not included, because the updated emissions were not available for the year 2011 in the currently
7 applied GEOS-CHEM version.

8

9 **References**

10 Athanasopoulou, E., Tombrou, M., Pandis, S. N. and Russell, A. G.: The role of sea-salt
11 emissions and heterogeneous chemistry in the air quality of polluted coastal areas, *Atmos.*
12 *Chem. Phys.*, 8(19), 5755–5769, doi:10.5194/acp-8-5755-2008, 2008.

13 Athanasopoulou, E., Tombrou, M., Russell, A. G., Karanasiou, A., Eleftheriadis, K. and
14 Dandou, A.: Implementation of road and soil dust emission parameterizations in the aerosol
15 model CAMx: Applications over the greater Athens urban area affected by natural sources,
16 *Journal of Geophysical Research: Atmospheres*, 115(D17), n/a–n/a,
17 doi:10.1029/2009JD013207, 2010.

18 Bergström, R., Denier van der Gon, H. A. C., Prévôt, A. S. H., Yttri, K. E. and Simpson, D.:
19 Modelling of organic aerosols over Europe (2002–2007) using a volatility basis set (VBS)
20 framework: application of different assumptions regarding the formation of secondary organic
21 aerosol, *Atmos. Chem. Phys.*, 12(18), 8499–8527, doi:10.5194/acp-12-8499-2012, 2012.

22 Bey, I., Jacob, D. J., Yantosca, R. M., Logan, J. A., Field, B. D., Fiore, A. M., Li, Q., Liu, H.
23 Y., Mickley, L. J. and Schultz, M. G.: Global modeling of tropospheric chemistry with
24 assimilated meteorology: Model description and evaluation, *J. Geophys. Res.*, 106(D19),
25 23073–23095, doi:10.1029/2001JD000807, 2001.

26 Bieser, J., Aulinger, A., Matthias, V., Quante, M., and Denier van der Gon, H.: Vertical
27 emission profiles for Europe based on plume rise calculations., *Environ. Pollut.*, 159, 2935–
28 2946, doi:10.1016/j.envpol.2011.04.030, 2011.

29 Bossioli, E., Tombrou, M., and Pilinis, C.: Adapting the Speciation of the VOCs Emission
30 Inventory, in the Greater Athens Area, *Water Air Soil Poll., Focus*, 2(5–6), 141–153, 2002.

31 Boylan, J. W. and Russell, A. G.: PM and light extinction model performance metrics, goals,

1 and criteria for three-dimensional air quality models, *Atmospheric Environment*, 40(26),
2 4946–4959, doi:10.1016/j.atmosenv.2005.09.087, 2006.

3 Brown, S. G., Lee, T., Roberts, P. T. and Collett, J. L.: Variations in the OM/OC ratio of
4 urban organic aerosol next to a major roadway, *Journal of the Air & Waste Management*
5 *Association*, 63(12), 1422–1433, doi:10.1080/10962247.2013.826602, 2013.

6 Chin, M., Rood, R. B., Lin, S.J., Müller, J.F., and Thompson, A. M.: Atmospheric sulfur cycle
7 in the global model GOCART: Model description and global properties, *J. Geophys. Res.*, 105,
8 24,661–24,687, 2000.

9 Chung, S. H. and Seinfeld, J. H.: Global distribution and climate forcing of carbonaceous
10 aerosols, *J. Geophys. Res.*, 107(D19), 4407, doi:10.1029/2001JD001397, 2002.

11 Dandou A., Tombrou M., Kalogiros J., Bossioli E., Bezantakos S., Biskos G., Kouvarakis
12 G.N., Mihalopoulos N., Allan J., Coe H. 2014 Simulation of Marine Boundary Layer
13 Evolution in the Aegean Sea during Etesians, COMECAP2014 e-book of proceedings ISBN:
14 978-960-524-430-9 Vol 1, pp. 220-224

15 Emery C, Tai E, Yarwood G (2001) Enhanced meteorological modeling and performance
16 evaluation for two Texas Ozone Episodes, Report to the Texas Natural Resources
17 Conservation Commission, prepared by ENVIRON, International Corp., Novato, CA

18 Fountoukis, C. and Nenes, A.: ISORROPIA II: a computationally efficient thermodynamic
19 equilibrium model for K^+ – Ca^{2+} – Mg^{2+} – NH_4^+ – Na^+ – SO_4^{2-} – NO_3^- – Cl^- – H_2O aerosols,
20 *Atmos. Chem. Phys.*, 7(17), 4639–4659, doi:10.5194/acp-7-4639-2007, 2007.

21 Guenther, A., Karl, T., Harley, P., Wiedinmyer, C., Palmer, P. I., and Geron, C.: Estimates of
22 global terrestrial isoprene emissions using MEGAN (Model of Emissions of Gases and
23 Aerosols from Nature), *Atmos. Chem. Phys.*, 6, 3181–3210, doi:10.5194/acp-6-3181-2006,
24 2006.

25 Henze, D. K., Seinfeld, J. H., Ng, N. L., Kroll, J. H., Fu, T.-M., Jacob, D. J. and Heald, C. L.:
26 Global modeling of secondary organic aerosol formation from aromatic hydrocarbons: high-
27 vs. low-yield pathways, *Atmos. Chem. Phys.*, 8(9), 2405–2420, doi:10.5194/acp-8-2405-
28 2008, 2008.

29 Hong S-Y, Noh Y, Dudhia J (2006) A new vertical diffusion package with an explicit
30 treatment of entrainment processes. *Mon Weather Rev* 134:2318–2341

1 Im, U., Markakis, K., Koçak, M., Gerasopoulos, E., Daskalakis, N., Mihalopoulos, N.,
2 Poupkou, A., Kindap, T., Unal, A. and Kanakidou, M.: Summertime aerosol chemical
3 composition in the Eastern Mediterranean and its sensitivity to temperature, *Atmospheric*
4 *Environment*, 50, 164–173, doi:10.1016/j.atmosenv.2011.12.044, 2012.

5 Kanakidou, M., Mihalopoulos, N., Kindap, T., Im, U., Vrekoussis, M., Gerasopoulos, E.,
6 Dermitzaki, E., Unal, A., Koçak, M., Markakis, K., Melas, D., Kouvarakis, G., Youssef, A. F.,
7 Richter, A., Hatzianastassiou, N., Hilboll, A., Ebojie, F., Wittrock, F., von Savigny, C.,
8 Burrows, J. P., Ladstaetter-Weissenmayer, A. and Moubasher, H.: Megacities as hot spots of
9 air pollution in the East Mediterranean, *Atmospheric Environment*, 45(6), 1223–1235,
10 doi:10.1016/j.atmosenv.2010.11.048, 2011.

11 Kopanakis, I., Eleftheriadis, K., Mihalopoulos, N., Lydakis-Simantiris, N., Katsivela, E.,
12 Pentari, D., Zarnpas, P. and Lazaridis, M.: Physico-chemical characteristics of particulate
13 matter in the Eastern Mediterranean, *Atmospheric Research*, 106, 93–107,
14 doi:10.1016/j.atmosres.2011.11.011, 2012.

15 Mailler, S., Khvorostyanov, D. and Menut, L.: Impact of the vertical emission profiles on
16 background gas-phase pollution simulated from the EMEP emissions over Europe, *Atmos.*
17 *Chem. Phys.*, 13(12), 5987–5998, doi:10.5194/acp-13-5987-2013, 2013.

18 Price, C. and Rind, D.: A Simple lightning parameterization for calculating global lightning
19 distributions. *J. Geophys. Res.*, 97(D9), 9919-9933, doi:10.1029/92JD00719, 1992.

20 Protonotariou A, Bossioli E, Tombrou M, Bossioli E, Mihalopoulos N, Biskos G, Kalogiros
21 J, Kouvarakis G. Amiridis V (2013) Air Pollution in Eastern Mediterranean: Nested-Grid
22 GEOS-CHEM Model Results and Airborne Observations, *Springer Atmos. Sci.*3: 1203-1209,
23 DOI: 10.1007/978-3-642-29172-2_168

24 Skamarock, W. C., Klemp, J. B., Dudhia, J., Gill, D. O., Barker, D. M., Wang, W. and
25 Powers, J. G.: A Description of the Advanced Research WRF Version 3, NCAR Technical
26 Note TN-468+STR., 113 pp, 2008.

27 Tagaris, E., Sotiropoulou, R. E. P., Gounaris, N., Andronopoulos, S. and Vlachogiannis, D.:
28 Air quality over Europe: modelling gaseous and particulate pollutants, *Atmos. Chem. Phys.*,
29 13(18), 9661–9673, doi:10.5194/acp-13-9661-2013, 2013.

30 Tesche TW, McNally DE, Emery CA, Tai E (2001) Evaluation of the MM5 model over the
31 Midwestern U.S. for three 8-hr oxidant episodes. Prepared for the Kansas City Ozone

1 Technical Work Group, prepared by Alpine Geophysics, LLC, Ft. Wright, KY and
2 ENVIRON International Corp., Novato, CA

3 Tombrou M, E Bossioli, AP Protonotariou, H Flocas, C Giannakopoulos, A Dandou (2009)
4 Coupling GEOS-CHEM with a regional air pollution model for Greece. *Atmos. Environ.*,
5 doi:10.1016/j.atmosenv.2009.04.003 Tombrou, M., Bossioli, E., Kalogiros, J., Allan, J. D.,
6 Bacak, A., Biskos, G., Coe, H., Dandou, A., Kouvarakis, G., Mihalopoulos, N., Percival, C. J.,
7 Protonotariou, A. P. and Szabó-Takács, B.: Physical and chemical processes of air masses in
8 the Aegean Sea during Etesians: Aegean-GAME airborne campaign, *Science of The Total*
9 *Environment*, 506–507, 201–216, doi:10.1016/j.scitotenv.2014.10.098, 2015.

10 Turpin, B. J. and Lim, H.-J.: Species Contributions to PM_{2.5} Mass Concentrations: Revisiting
11 Common Assumptions for Estimating Organic Mass, *Aerosol Science and Technology*, 35(1),
12 602–610, doi:10.1080/02786820119445, 2001.

13 Vestreng, V., and Klein, H.: Emission data reported to UN-ECE/EMEP: Quality assurance
14 and trend analysis & presentation of WebDab, Norwegian Meteorological Institute, Oslo,
15 Norway, 2002.

16 Yevich, R. and Logan, J. A.: An assessment of biofuel use and burning of agricultural waste
17 in the developing world, *Global Biogeochem. Cycles*, 17(4), 1095,
18 doi:10.1029/2002GB001952, 2003

1 Table S1. Emission rates for the gaseous and aerosol species in PM₄₀. Numbers correspond to
 2 daily sums (summer weekday) for each of the two countries within the PMCAMx simulation
 3 domain.

Gas and aerosol (PM ₄₀) species		Total emission rates			
		Greece		Turkey	
		Area sources	Point sources	Area sources	Point sources
Gases (megamols day ⁻¹)	Carbon monoxide	140	9.2	51	54
	Sulfur dioxide	3.4	27	0.2	45
	Nitric oxide	44	5.7	12	35
	Nitrogen dioxide	3.2	0.8	0.8	2.5
	Ammonia	35	-	34	0.6
	Non-methane hydrocarbons	52	0.9	37	0.6
	Large chain hydrocarbons	0.5	-	0.2	-
Aerosol components (tons day ⁻¹)	Organics	31	9	16	17
	Sulfate	362	522	14	38
	Elemental carbon	61	47	28	13
	Sodium chloride ^a	23,867	-	23,867	-
	Crustal species ^b	750	-	750	-
	Rest aerosol components (species not treated by the PMCAMx)	703	210	2.6	219
	Nitrate ^c	0.029	-	0.011	-

4 ^aSodium chloride corresponds mainly to sea-salt emissions of the whole simulation domain, developed
 5 as described in Athanasopoulou et al. (2008). It is noted that sea-salt emissions are calculated online
 6 with meteorology, thus they differ from day-to-day. This value corresponds to the date 29 August
 7 2011.

8 ^b Aeolian soil dust emissions (mainly calcium, potassium, magnesium) from the whole simulation
 9 domain are calculated online with meteorology, thus they differ from day-to-day (Athanasopoulou et
 10 al., 2010). This value corresponds to the date 29 August 2011.

11 ^c Nitrate is only produced due to road dust re-suspension (Athanasopoulou et al., 2010).

1 Table S2. Mathematical formulation and statistical benchmarks, goals and criteria for
 2 evaluating the model system used in this study.

Metrics	Formulas ^a	Benchmarks, Goals, Criteria	Notes
Mean Bias	$MB = \frac{1}{N} \sum_{i=1}^N (E_i - O_i)$	$\leq \pm 0.1 \text{g/kg}, \leq \pm 0.5 \text{K}, \leq \pm 10 \text{deg}, \leq \pm 0.5 \text{m/s}$	
Mean Absolute Gross Error	$MAGE = \frac{1}{N} \sum_{i=1}^N E_i - O_i $	$< 2 \text{g/kg}, \leq 2 \text{K}, \leq 30 \text{deg}, -$	Statistical benchmarks for water vapor mixing ratio, air temperature, wind direction and wind speed, respectively (Tesche et al., 2001; Emery et al., 2001).
Root Mean Square Error	$RMSE = \sqrt{\frac{1}{N} \sum_{i=1}^N E_i - O_i ^2}$	$-, -, -, \leq 2 \text{m/s}$	
Index of Agreement	$IA = 1 - \left[\frac{N \cdot RMSE^2}{\sum_{i=1}^N (E_i - \bar{O} + O_i - \bar{O})^2} \right]$	$\geq 0.6, \geq 0.8, -, \geq 0.6$	
Mean Fractional Bias	$MFB = \frac{1}{N} \sum_{i=1}^N \frac{(E - O)}{\left(\frac{O + E}{2}\right)} 100\%$	$\pm 30, \pm 64, \pm 47, \pm 187, \pm 32, \pm 31, \pm 122, \pm 30$ (goals ^b) $\pm 60, \pm 88, \pm 74, \pm 189, \pm 62, \pm 61, \pm 135, \pm 60$ (criteria ^b)	
Mean Fractional Error	$MFE = \frac{1}{N} \sum_{i=1}^N \frac{ E - O }{\left(\frac{O + E}{2}\right)} 100\%$	$50, 101, 83, 192, 58, 56, 149, 50$ (goals ^b) $75, 118, 102, 193, 81, 80, 158, 75$ (criteria ^b)	
Normalized Mean Bias	$NMB = \frac{1}{N} \sum_{i=1}^N \frac{(E_i - O_i)}{O_i} 100\%$		
Normalized Mean Error	$NME = \frac{1}{N} \sum_{i=1}^N \frac{ E_i - O_i }{O_i} 100\%$		
Correlation coefficient	$r = \left[\frac{\sum_{i=1}^N (E_i - \bar{E})(O_i - \bar{O})}{\sum_{i=1}^N (E_i - \bar{E}) \sum_{i=1}^N (O_i - \bar{O})} \right]$		
Standard deviation	$Stdev = \sqrt{\frac{1}{N} \sum_{i=1}^N x_i - \bar{x} ^2}$		x_i and \bar{x} are the raw and mean estimation or observation values

3 ^a E is the estimated (modeled) and O is the observed value of each parameter, paired in space and time
 4 for each i of N data pairs. \bar{E} and \bar{O} are the mean values of estimations and observations, respectively.

5 ^b The goals and criteria for aerosol components are given by the equations below (Boylan and Russell,
 6 2006):

7 $MFB = \pm 170 e^{-0.5 \left(\frac{\bar{O} + \bar{E}}{0.5}\right) + 30}$ and $MFE = 150 e^{-0.5 \left(\frac{\bar{O} + \bar{E}}{0.75}\right) + 50}$ (goals),

8 $MFB = \pm 140 e^{-0.5 \left(\frac{\bar{O} + \bar{E}}{0.5}\right) + 60}$ and $MFE = 125 e^{-0.5 \left(\frac{\bar{O} + \bar{E}}{0.75}\right) + 75}$ (criteria), where \bar{E} and \bar{O} are the mean
 9 values of estimations and observations, respectively.

Table S3. Prediction skill metrics of the basic meteorological parameters and submicron aerosol concentrations (**prd**, in **bold**) against airborne measurements (obs) from the nine flights during the period of interest (29 August – 09 September 2011). Performance metrics with **green** (**red**) fonts indicate **good** (**poor**) model performance, according to the selected criteria of evaluation, given in Table S2. The rest model outputs (performance metrics with black fonts) are acceptable (average model performance).

Metrics	Water vapor mixing ratio g/kg	Temperature K	Wind speed m/s	Wind direction deg	Sulfate	Nitrate	Ammonium	Chloride	Organics
					$\mu\text{g m}^{-3}$ (below/above 2.2 km asl)				
Mean prd	4.2	278.9	8.0		4.8 (5.5/3.8)	0.9 (1.9/0.4)	1.1 (1.7/0.5)	0.02 (0.05/0)	1.4 (2.3/0.9)
Mean obs	4.2	279.2	8.4		5.0 (5.8/3.7)	0.1 (0.2/0.04)	1.0 (1.5/0.5)	0.01 (0.02/0)	2.4 (4.4/1.1)
Max prd	14.2	300.3	19.5		12.1 (12.1/9.7)	7.9 (7.9/2.7)	4.2 (4.2/1.5)	0.4 (0.4/0.03)	6.8 (6.8/4.8)
Max obs	14.4	304.2	24.1		23.4 (23.4/15.0)	1.9 (1.9/1.5)	5.2 (5.2/2.5)	0.8 (0.3/0.8)	10.7 (10.7/9.4)
Stdev prd	3.7	11.7	2.9		2.4 (2.4/2.2)	1.5 (2.1/0.4)	0.8 (0.8/0.4)	0.07 (0.1/0)	1.3 (1.4/0.9)
Stdev obs	3.9	11.1	4.1		3.8 (3.8/3.4)	0.1 (0.1/0.1)	0.9 (0.8/0.5)	0.03 (0.03/0.03)	2.5 (2.2/1.9)
IA	0.96	0.99	0.70		-	-	-	-	-
MB	0.05	-0.26	-0.40	8.07	-0.2 (-0.3/0.1)	0.8 (1.7/0.3)	0.1 (0.2/-0.02)	0.01 (0.03/0)	-0.9 (-2.1/-0.2)
MAGE	1.10	1.63		23.44	2.2 (2.4/1.8)	0.9 (1.9/0.4)	0.6 (0.8/0.3)	0.03 (0.1/0)	1.4 (2.2/0.8)
RMSE			3.64		3.1 (3.5/2.4)	1.7 (2.7/0.6)	0.8 (1.0/0.4)	0.07 (0.1/0.03)	2.0 (2.7/1.3)
MFB (%)					20.4 (6.0/41.2)	67.8 (17.1/93.8)	21.9 (17.0/27.1)	-150.1 (-74.7/-194.3)	2.0 (-64.2/42.9)
MFE (%)					55.2 (43.8/71.6)	184.0 (173.7/189.3)	63.4 (57.4/69.9)	18.3 (162.2/-65.7)	83.3 (74.5/88.7)
NMB (%)					-0.03 (-0.06/0.02)	9.3 (9.3/9.1)	0.1 (0.1/-0.03)	1.8 (1.3/-2.7)	-0.4 (-0.5/-0.2)
NME (%)					0.4 (0.4/0.5)	10.3 (10.2/10.5)	0.6 (0.6/0.6)	3.9 (2.7/-7.7)	0.6 (0.5/0.7)
r					0.6 (0.4/0.7)	0.3 (-0.1/-0.1)	0.6 (0.2/0.6)	0.2 (0.1/0.03)	0.8 (0.6/0.8)

r^2					0.3 (0.2/0.5)	0.1 (0.01/0.01)	0.3 (0.03/0.4)	0.03(0/0)	0.6 (0.4/0.6)
% within a factor of 2					70.2 (79.8/56.4)	4.5 (3.7/4.9)	59.2 (65.1/52.9)	6.6 (3.7/8.3)	41.9 (48.2/37.9)
No of samples	16052	16052	16052	15133	1335 (787/548)	2244 (765/1479)	1518 (788/730)	1624 (599/1025)	2066 (788/1278)

Table S4. Prediction skill metrics of the aerosol concentrations (**prd**, in **bold**) against ground measurements (obs) during the period of interest (29 August – 09 September 2011). MFB and MFE with **green** fonts indicate **good** model performance, according to the selected criteria of evaluation, given in Table S2.

Metrics	PM ₁ Sulfate	PM ₁₀ OC ^a μgm ⁻³ Vigla (N. Aegean) / Finokalia (S. Aegean)	PM ₁₀ EC	PM ₁₀
Mean prd	-/ 6.4	2.0/2.1	0.32/0.26	-/29.1
Mean obs	-/5.9	2.3/2.9	0.25/0.38	-/30.6
Max prd	-/12.5	4.8/4.3	0.6/0.4	-/47.8
Max obs	-/14.3	5.0/8.1	0.8/1.2	-/59.8
Stdev prd	-/3.1	1.0/0.8	0.13/0.0.8	-/8.6
Stdev obs	-/3.5	1.1/1.3	0.20/0.23	-/12.8
MB	-/0.5	-0.2/-0.8	0.07/-0.12	-/1.5
MAGE	-/2.4	0.7/1.2	0.16/0.19	-/13.9
RMSE	-/2.9	0.9/1.5	0.21/0.27	-/17.9
MFB (%)	-/12.9	-11.3/-28.2	40.8/-18.6	-/10.6
MFE (%)	-/45.1	36.6/46.1	63.1/55.6	-/47.4
NMB (%)	-/0.1	-0.1/-0.3	0.3/-0.3	-/0.0
NME (%)	-/0.4	0.3/0.4	0.7/0.5	-/0.5
r	-/0.6	0.6/0.2	0.3/0.1	-/-0.4
r ²	-/0.4	0.4/0.05	0.1/0.0	-/0.2
% within a factor of 2	-/78.8	83.9/80.9	54.8/71.4	-/76.9
No of samples	-/184	31/42	31/42	-/26

^a Organic aerosol predictions are divided by 2.1 (Turpin and Lim, 2001), to extract the carbon mass (OC).

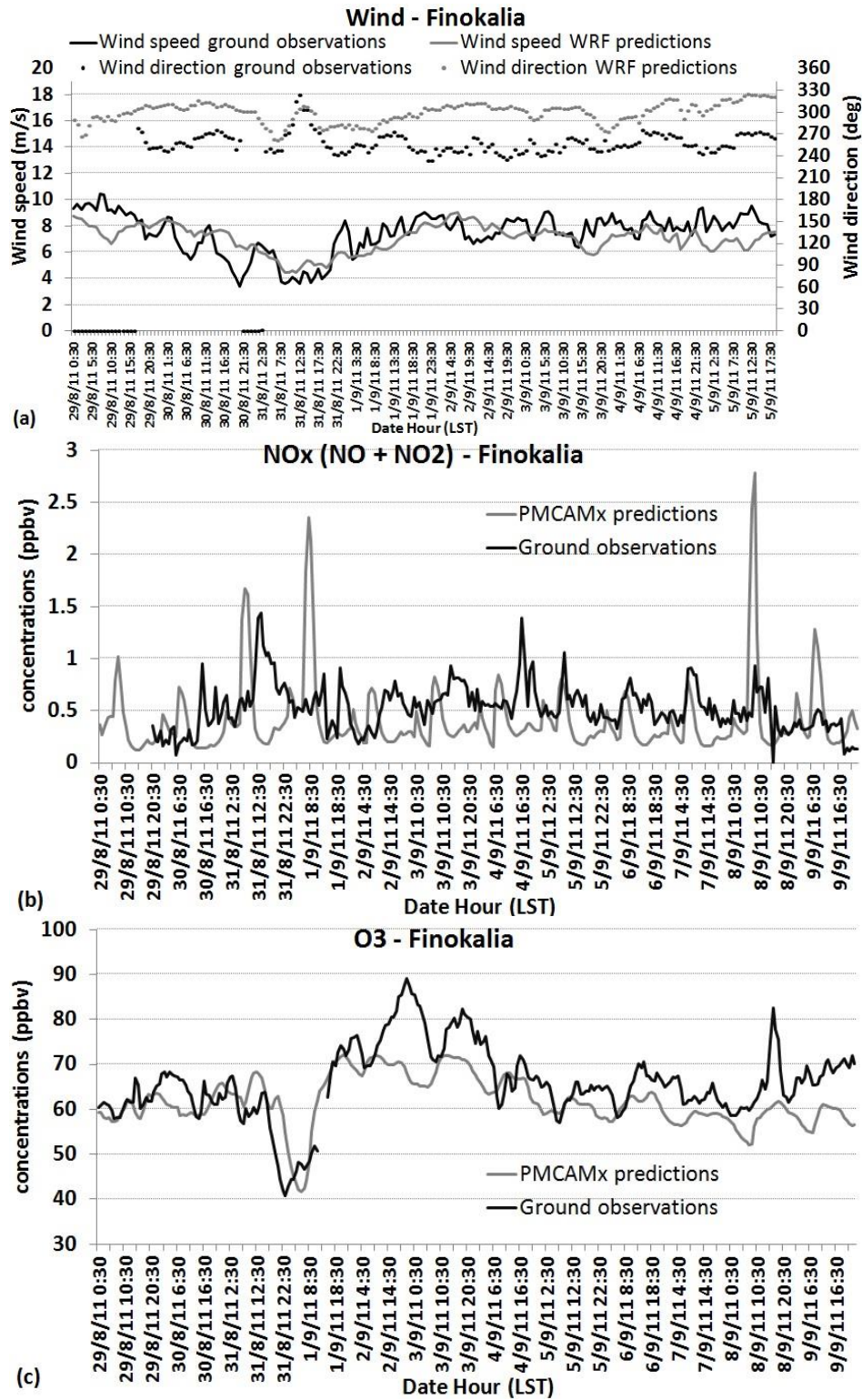


Figure S1. Comparison of predictions (grey) with hourly measurements (black) of: (a) wind speed (m s^{-1}) and wind direction (deg), (b) NO_x concentrations (ppbv) and (c) O_3 concentrations (ppbv) over Finokalia (Crete).

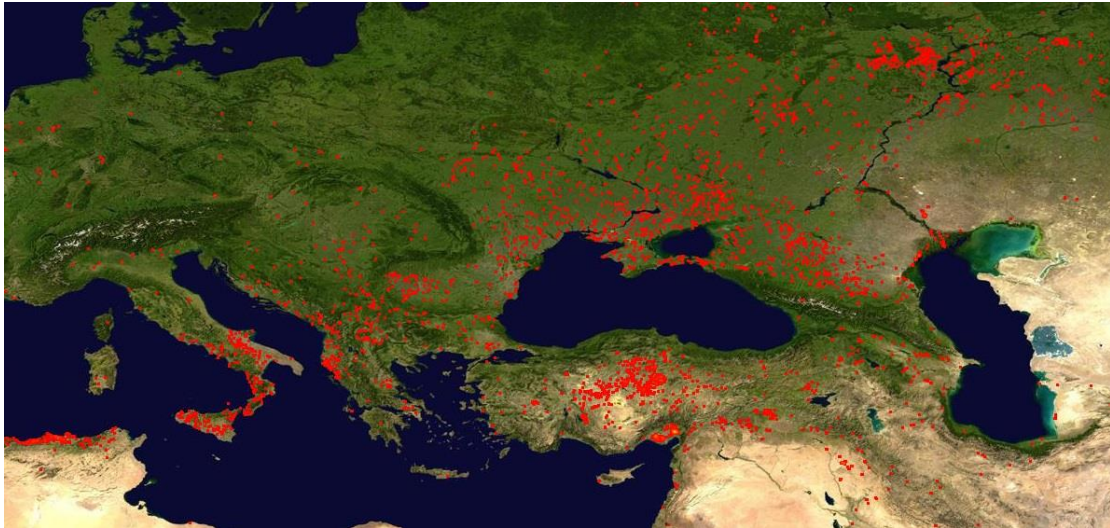


Figure S2. MODIS image acquisition, showing the fire events in Turkey, south and east Europe from 29 August until 07 September 2011.